Marine Pollution Bulletin 160 (2020) 111678

Contents lists available at ScienceDirect

Marine Pollution Bulletin

journal homepage: www.elsevier.com/locate/marpolbul

Fate of river-borne floating litter during the flooding event in the northeastern part of the Black Sea in October 2018

Evgeniya Korshenko[a,b,*], Victor Zhurbas[b], Alexander Osadchiev[b], Pelagiya Belyakova[c]

[a] N.N. Zubov State Oceanographic Institute, Roshydromet, 119034 Moscow, Kropotkinskiy Lane 6, Russian Federation
[b] Shirshov Institute of Oceanology, Russian Academy of Sciences, 117997 Moscow, Nahimovskiy Prospect 36, Russian Federation
[c] Water Problems Institute, Russian Academy of Sciences, 119333 Moscow, Gubkina Street 3, Russian Federation

ARTICLE INFO

Keywords:
Floating marine litter
River plume
Convergence zone
Rain-induced flood
Coastal water quality
Black Sea

ABSTRACT

This study is focused on delivery and fate of floating marine litter (FML) carried by rivers to coastal sea. We examine a large flooding event which happened in the northeastern part of the Black Sea in October 2018. A high resolution circulation model coupled with a Lagrangian particle model is applied to simulate transport of riverine FML in the coastal sea. During this flood multiple river plumes in the study area coalesced into one stripe of freshened water which occupied large segment of coastal sea along the shoreline. Riverine FML was transported within this stripe far off its sources in river mouths and remained arrested near the shore. As a result, approximately half of the discharged FML was washed ashore by the Stokes drift. FML, which remained in the sea, accumulated at convergence lines associated with large salinity gradients at the fronts between the river plumes and the ambient sea.

1. Introduction

Marine litter is one of the leading threats to the marine environment that has been growing worldwide over the past several decades. This is especially true for plastic litter due to its durability that results in the ubiquitous presence of plastic in the ocean. Nowadays, plastic litter accounts for the major part of marine litter and can be considered as a 'common concern of humankind' (UNEP, 2016). The widely quoted report about total mass of the plastic litter in the ocean predicts it to become of the same order as the total mass of fish by the middle of this century (World Economic Forum and Ellen MacArthur Foundation, 2016). This estimation is not yet verifiable but can be quite indicative of the modern and potential future state of marine plastic pollution. The increasing plastic pollution was detected at sea surface, pelagic, and benthic oceanic zones, sea ice, and sea shore (Barnes et al., 2009; Moore, 2008; Avio et al., 2017). Many works were devoted to the negative impact of plastic litter on the marine environment including ingestion by marine animals (Avio et al., 2015; Courtene-Jones et al., 2017; La Beur et al., 2019), entanglement of marine animals (Page et al., 2004; Votier et al., 2011; Moore et al., 2009; Gregory, 2009), absorption of toxic pollutants (Hirai et al., 2011; Rochman et al., 2014), and introduction of invasive species (Derraik, 2002; Barnes, 2002; Zettler et al., 2013). As a result, understanding of delivery, transport, and transformation of plastic litter in the ocean is an issue of paramount importance and requires specific studies (Chubarenko et al., 2020; Coyle et al., 2020).

Shorelines, wastewater pipelines, and especially rivers are considered to be the major land-based sources of marine plastic pollution. Total annual inputs of riverine plastic litter into the ocean are estimated as 0.41–4 million tonnes (Schmidt et al., 2017) or 1.15–2.41 million tonnes (Lebreton et al., 2017). The role of rivers in delivery of marine litter is crucial for many coastal areas all over the World. In particular, inputs from only ten large and heavily polluted rivers located in southern and south-eastern Asia and in Africa provide 67–95% of total global volume of the riverine plastic pollution (Lebreton et al., 2017; Schmidt et al., 2017).

The global production of plastic is increasing every year and it reached almost 360 million tonnes in 2018 (PlasticsEurope, 2019). The most common plastic polymers include polyethylene (PE), polypropylene (PP), polystyrene (PS), polyvinyl chloride (PVC), polyethylene terephthalate (PET), and polyurethane (PUR) resins. By mass roughly half of all produced plastics have low density, as compared to seawater, and can float at sea surface (Geyer et al., 2017). However, floating characteristics of plastic items depend on external factors (e.g., trapped air, biofouling, shape), so many PS particles, which typical density (1.04–1.05 g/cm^3) is slightly greater than that of sea water, also float at sea surface (Van Sebille et al., 2020). It is considered that PE, PP and PS dominate in floating marine litter (FML). FML is observed

* Corresponding author at: 119034 Moscow, Kropotkinsky Lane 6, Russian Federation.
E-mail addresses: zhenyakorshenko@gmail.com (E. Korshenko), zhurbas@ocean.ru (V. Zhurbas), osadchiev@ocean.ru (A. Osadchiev).

https://doi.org/10.1016/j.marpolbul.2020.111678
Received 12 April 2020; Received in revised form 10 September 2020; Accepted 11 September 2020
Available online 06 October 2020

everywhere in the ocean, however, its spatial distribution shows significant inhomogeneity due to its dependence on proximity and density of urban population, coastal and marine economic activities, winds, sea currents, etc. (Galgani et al., 2015; Cózar et al., 2017). Several evident accumulation zones of FML were formed in the recent decades including five well-known sub-tropical gyres in the Pacific, Atlantic, and Indian oceans (Eriksen et al., 2014; Law et al., 2010, 2014; Maximenko et al., 2012), the enclosed Mediterranean and Black seas (Cózar et al., 2015; Suaria and Aliani, 2014; BSC, 2019). Apart from these large-scale accumulation areas, marine debris retain in coastal environments for a long time (Lebreton et al., 2019). As a result, multiple accumulation zones of FML were registered at coastal areas which exhibit strong anthropogenic pressure (Galgani et al., 2015; Reisser et al., 2013; Ryan, 2013; Bagaev et al., 2018). In general, most coastal sea areas where marine litter has large residence time can be considered as areas of FML accumulation.

Many works were devoted to different aspects of hydrosphere plastic pollution during the last 10 years. The majority of these works were focused on, first, delivery of plastic litter by rivers (Wagner et al., 2014; Eerkes-Medrano et al., 2015; Horton et al., 2017) and, second, spreading of plastic litter in the ocean (Van der Wal et al., 2015; Bruge et al., 2018). However, very little attention was paid to the processes associated with plastic litter after it was discharged from rivers to sea and before it reached open sea, i.e., spreading and transformation of plastic litter in estuarine and coastal sea areas. In particular, we are aware of only few works focused on transport of FML within river plumes formed as a result of mixing between freshened river discharge and saline sea water (Atwood et al., 2019; Rech et al., 2014; Cheung et al., 2016; Ourmieres et al., 2018). Dynamics of river plumes is significantly different from dynamics of ambient sea that strongly affects spreading of FML. Generally, river plumes form shallow surface-advected layers, which can spread far off river mouths as a result of wind forcing or within coastal buoyancy currents (Horner-Devine et al., 2015). Due to large density gradients formed between river plumes and subjacent sea, as well as intense turbidity at this layer caused by large velocity shear suspended particles (including plastic litter) remain in the surface layer for a longer time, as compared to ambient sea. As a result, plastic litter accumulated in river plumes is effectively transported off river mouths to open sea, as compared to marine plastic litter delivered from seashore by winds or tides.

Many previous studies addressed marine litter floating in the Black Sea and trapped at the sea shore (Topçu et al., 2013; Suaria et al., 2015; Moncheva et al., 2016; Bat et al., 2017; Simeonova et al., 2017; Terzi and Seyhan, 2017; BSC, 2019; Stanev and Ricker, 2019; Miladinova et al., 2020). Recent numerical modelling studies by Stanev and Ricker (2019) and Miladinova et al. (2020) demonstrated presence of FML accumulation area in the northwestern and western part of the Black Sea, while strong temporal variability of surface circulation of the Black Sea prevents accumulation of FML in the central part of the sea. However, only large rivers inflowing to the Black Sea were considered in these studies, while the role of numerous small rivers was neglected.

The current study is focused on delivery and fate of FML which is discharged from rivers at the northeastern part of the Black Sea. Many rivers inflow to the considered coastal area from multiple gorges of the Western Caucasus (Fig. 1). More than 1.1 million people live at the territory drained by these rivers resulting in strong anthropogenic pressure to the local environment (Balabanov et al., 2011; Alexeevsky et al., 2016). These rivers are relatively small, their total annual discharge is estimated as 6.5–7.5 km^3 (Jaoshvili, 2002; Alexeevsky et al., 2016). Nevertheless, they are considered to be the main source of marine litter in the study area especially during rain-induced flooding events that can occur up to 25 times a year. During these short-term events runoff from small rivers can abruptly increase by 1–2 orders of magnitude, as compared to the average climatic conditions. Water level in these rivers rises, they overflow the banks and carry a large amount of riverine floating matter into the sea (Alexeevsky et al., 2016). As a result, river plumes, first, determine spreading of FML in the considered coastal area and, second, play the role of the transition zone for plastic pollution between the rivers and open sea.

In the present study we examine a large flooding event which happened in the northeastern part of the Black Sea in October 2018. We reconstruct spreading patterns of FML at the coastal sea area and detect areas of its accumulation at seacoast caused by washing ashore. Dynamics of coastal circulation and river plumes in the study area were explicitly described and discussed in a number of previous studies (Korotkina et al., 2011, 2014; Zavialov et al., 2014; Osadchiev, 2015; Osadchiev and Korshenko, 2017; Osadchiev, 2018; Osadchiev and Sedakov, 2019). The northeastern coast of the Black Sea is regularly observed within numerous monitoring programs devoted to prevent, reduce, and mitigate impacts of marine pollution (BSC, 2007, 2019). However, no quantitative information of river-borne litter (including FML) and its influence on coastal sea areas was published yet. Also we are not aware of any study focused on FML fate along the densely populated northeastern coast of the Black Sea which is governed by spreading of local river plumes. Therefore, the results obtained in this study hold promise to provide improved quantitative assessments and new insights into monitoring, modelling, and forecasting of marine plastic pollution in the study area, as well as in many coastal regions in the World.

The study is organized as follows. Information about the satellite and in situ data used in this study is provided in Section 2. Section 3 describes numerical models used to simulate the transport of riverine floating matter in the coastal sea. The description of numerical simulation results, including FML transport, accumulation, and washing ashore is given in Section 4. The summary and conclusions are presented in Section 5.

2. Material and methods

2.1. Satellite observations

We studied spreading dynamics of river plumes in the northeastern part of the Black Sea using Sentinel-2 MSI and Landsat 8 OLI data collected in October and November 2018 before, during, and after a large flooding event that occurred on 24–25 October 2018. The Landsat 8 Surface Reflectance Level-2 products with 30 m spatial resolution were downloaded from the United States Geological Survey web repository (http://earthexplorer.usgs.gov). The Sentinel-2 Level-1C products with 10 m spatial resolution were downloaded from the Copernicus Open Access Hub. Atmospheric correction was applied to these products using Sen2Cor module version 2.2.1 within the Sentinel-2 Toolbox (S2TBX), Sentinel Application Platform (SNAP) version 5.0.7.

2.2. River discharge

We examined plumes formed by 8 rivers in the study area: Mzymta (basin area of 839 km^2), Kudepsta (87.1 km^2), Khosta (98.5 km^2), Matsesta (67.5 km^2), Sochi (296 km^2), Dagomys (103 km^2), Shakhe (423 km^2), and Psezuapse (237 km^2). Freshwater discharge rates of these rivers and precipitation amounts one day before, during, and several days after the flooding event period (23–27 October 2018) were obtained from the Russian Hydrometeorological Service (https://gmvo.skniivh.ru/). The precipitation data consists of hourly measurements at 7 rain gauge stations at the study area. Discharge data consists of hourly discharge rates measured at gauge stations located near mouths of the Mzymta, Khosta, Sochi, Shakhe and Psezuapse rivers. Moreover, we used gauge data from the Zapadny Dagomys River (basin area of 47.1 km^2), which is the main tributary of the Dagomys River and accounts for a half of its drainage area and discharge. Discharge rates for the Kudepsta,

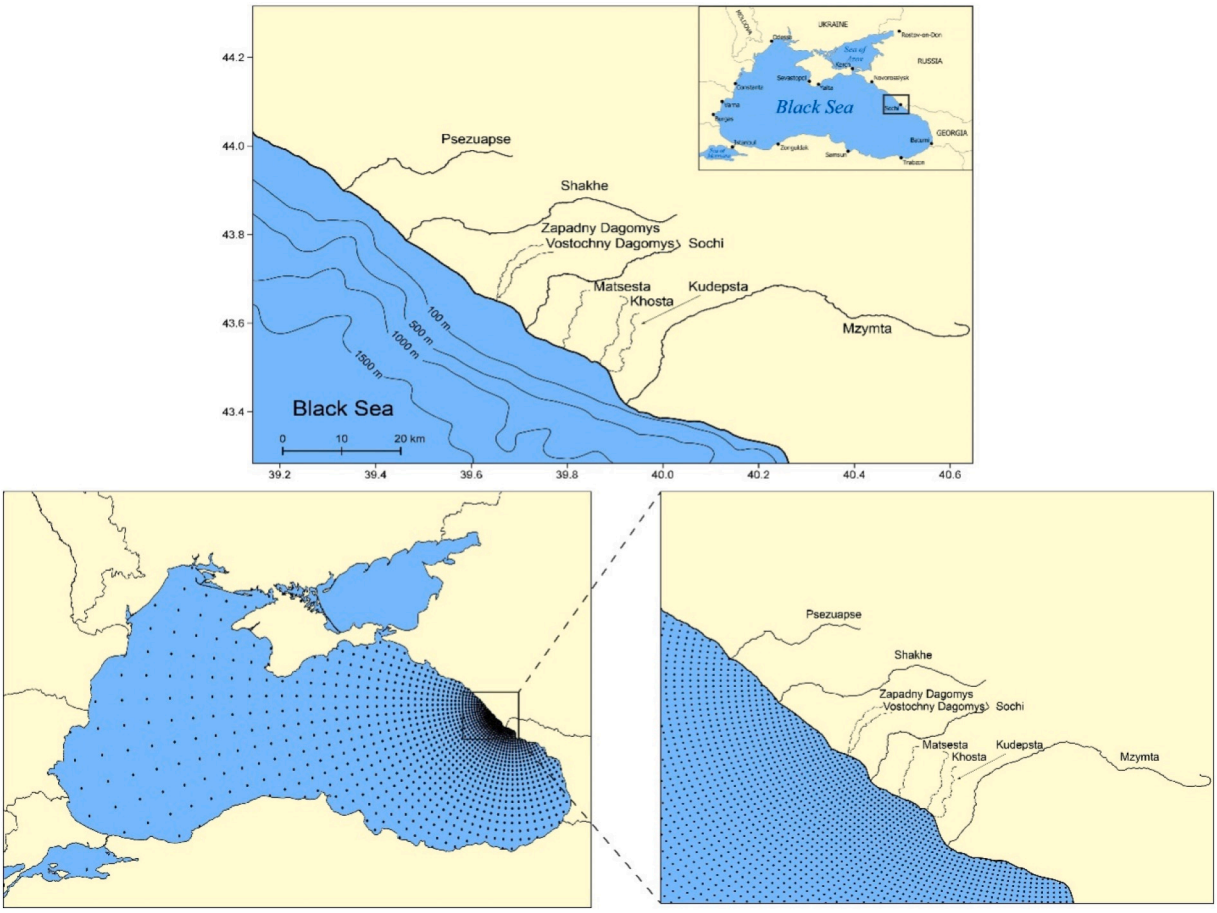

Fig. 1. Study area, bathymetry and locations of the rivers addressed in this study (top panel). Black box at the inset shows location of the study area at the northeastern part of the Black Sea. INMOM model domain at the Black Sea (every 15th grid point is shown) (left on bottom panel) and at the study area (every 5th grid point is shown) with indication of the location of the considered river estuaries (right on bottom panel).

Matsesta, and Dagomys rivers were evaluated using KW-GIUH model (Lee and Yen, 1997; Lee et al., 2009; Gonchukov et al., 2019).

KW-GIUH (Kinematic Wave-Geomorphologic Instantaneous Unit Hydrograph) (Lee and Yen, 1997; Lee et al., 2009) is an event-based rainfall-runoff model, which is an efficient tool for reconstructing hydrological response of a river catchment on intense precipitation events in case of sparse in situ data. The input data required for this model include lengths and slopes of river sub-catchments and channels, overland-flow roughness coefficients, and channel roughness coefficients. The related geomorphologic information was obtained from the HydroSHEDS (Hydrological data and maps based on SHuttle Elevation Derivatives at multiple Scales) (https://www.hydrosheds.org/) using ArcGIS tools. The required coefficients were calibrated against the flooding events that occurred on 25 June 2015 at the Khosta and Zapadny Dagomys rivers using hourly precipitation measurements from the nearest rain gauges. These coefficients were verified against the flooding event occurred during 24–25 October 2018. The simulated discharge peak differed from the observed discharge by 2–8%, while the time of the peak and the related flood volumes showed good agreement with the observed values.

The discharge rates for the Kudepsta, Matsesta, and Dagomys rivers were simulated by KW-GIUH model using precipitation data from the nearest rain gauges. The overland-flow roughness and channel roughness coefficients were prescribed the same as for the adjacent rivers (Khosta and Zapadny Dagomys). The simulated river hydrographs were additionally validated against the 10-minute water level data obtained from the Automated Flood Monitoring System of the Krasnodar Territory EMERCIT (http://www.emercit.com).

2.3. Circulation model setup (INMOM)

An Eulerian model of marine circulation INMOM (Institute of Numerical Mathematics Ocean Model) was applied to simulate circulation in the Black Sea for further reconstruction of delivery and fate of riverine floating particles in the coastal sea. INMOM is a three-dimensional σ-coordinate model based on the primitive equations of ocean circulation with Boussinesq and hydrostatic approximations (Volodin et al., 2010). The regional INMOM version presented in this study was used and validated in several studies focused on coastal circulation, river plumes, and transport of pollutants (Diansky et al., 2013; Osadchiev and Korshenko, 2017). A short description of the applied model and the input data is given below. More detailed information is presented in the Supplementary material - 1.

A high resolution regional INMOM version with a non-uniform horizontal grid covered the Black Sea basin excluding the Azov and Marmara seas (Fig. 1). Model bathymetry was set according to the GEBCO dataset with a spatial resolution of 15″ (www.gebco.net). Atmospheric forcing including turbulent heat, salt, and momentum fluxes was calculated from short- and long-wave radiation, air temperature, precipitation, relative humidity, sea level pressure, and wind data obtained from the regional atmospheric Weather Research and Forecast Model (WRF) (Skamarock et al., 2008) with spatial and temporal resolutions of 10 km and 1 h respectively.

Since three-dimensional monthly climatic mean fields were used for initial thermohaline conditions, the numerical simulation started on 1 January 2018, i.e., almost 10 months before the regarding flood event (24–25 October 2018). These thermohaline fields for the Black Sea with

a horizontal resolution of 0.1° × 0.0625° and with 36 vertical z-levels from 0 to 2150 m were provided by MHI RAS (Marine Hydrophysical Institute of the Russian Academy of Sciences) (Polonsky et al., 2013). These data were also used for corrections of sea surface salinity field.

Water transport through the Kerch and Bosporus straits that connect the Black Sea with the Azov and Marmara seas, as well as the discharge rates of the largest rivers inflowing to the Black Sea including the Danube, Dniester, Dnieper, Kodori, Rioni, Inguri, Yeshilirmak, Kyzylirmak, and Sakarya rivers were set according to the climatic runoff data (Jaoshvili, 2002).

To get quantitative estimations of the net effect of river plume dynamics during the flooding event on FML transport and its coastal accumulation caused by washing ashore, we performed two numerical experiments. In the first experiment the climatic runoff data from the Russian Hydrometeorological Service (https://gmvo.skniivh.ru/) was used for the main 8 rivers in the study area except for the period shortly before, during, and after the flooding event (23–27 October 2018) when the reconstructed hourly discharge rates were used. During the second experiment, only climatic runoff data was used, including the flooding event period, i.e., it simulated "no flood" conditions.

2.4. Setup of Lagrangian particles

The trajectories of Lagrangian floating particles, which reproduce spreading of FML, were calculated using simulated by INMOM current velocity field in the uppermost model layer. This field has temporal resolution of 30 min obtained by numerical integration of the plain equations of the Lagrangian particle advection with a Runge-Kutta scheme of higher order of accuracy (Väli et al., 2018). Velocities simulated by the INMOM on a non-uniform grid were interpolated to a uniform grid with 250 m × 250 m bins before calculating the trajectories. The particles were seeded in 250 m × 250 m grid bins corresponding to the mouths of the main rivers of the study area (Mzymta, Kudepsta, Khosta, Matsesta, Sochi, Dagomys, Shakhe, Psezuapse). The particles were released discretely in time by portions of N pieces per time step dt used for the Lagrangian velocity integration. The number of particles N released every dt seconds was set proportional to the actual value of river discharge rate: $N = \alpha Q dt$, where the proportionality factor α was chosen empirically as $\alpha = 0.001\ \mathrm{m}^{-3}$. The initial coordinates of particles were randomly generated with homogeneous probability distribution within the grid bin.

In order to study the influence of the Stokes drift on FML transport for both numerical experiments, we calculated trajectories of the Lagrangian floating particles with and without the Stokes drift. The BLKSEA_ANALYSIS_FORECAST_WAV_007_003 (Staneva et al., 2020) product containing hourly values of the Stokes drift velocities with a horizontal resolution of 0.028° × 0.037° was downloaded from the Copernicus Marine Environment Monitoring Service (https://marine.copernicus.eu/). The downloaded Stokes drift velocities were interpolated to a uniform grid with 250 m × 250 m bins and added to the velocities simulated by the INMOM. The accuracy of the particle tracking simulations was verified, the related results are presented in the Supplementary material - 1.

Apart from the Stokes drift, we decided to neglect windage effects, because the substantial share of FML consists of microplastic particles, e.g., fibers, small fragments of plastic bottles, films, bags, etc. These microplastic particles, in contrast to macroplastic items, are not elevated above sea surface and, therefore, do not experience any additional windage forcing.

3. Results

We analyzed cloud free optical satellite images acquired on 18, 28, 30, October and 2, 7, 19 November 2018 (Fig. 2). Good satellite imagery coverage of this period provided an opportunity to analyze the processes of spreading, coalescence, transformation, and dissipation of multiple river plumes formed in the study area during and after the considered flooding event.

Low discharge volumes during autumn drought resulted in small spatial scales (< 100 m) of river plumes observed on 18 October. Cloudy weather during the flooding event hindered satellite observations of the increased areas of the river plumes in response to the increased river discharges. Satellite image acquired on 28 October (Fig. 2a), i.e., one day after the end of the flooding event, showed multiple turbid river plumes formed along the shore. Cross-shore extents of the plumes increased to 1–5 km, the neighboring river plumes collided and coalesced along wide segments of the seashore. As a result, two 25–30 km long alongshore stripes of turbid water were observed in the northern and southern parts of the study area. During the next several days the northern stripe extended, its offshore scale increased to 5–7 km, while the southern stripe remained stable that was visible at satellite image acquired on 30 October (Fig. 2b). Steady dissipation of the freshened stripe as a result of mixing with the subjacent sea was accompanied by formation of multiple internal frontal zones, eddies, and meanders visible on 2 and 7 November (Fig. 2c). These features were associated with formation of the river plumes within the remnant freshened stripes and interaction of these stripes with coastal circulation. Final dissipation of the freshened stripe was observed on 19 November.

The flooding event considered in this study was caused by the heavy rainfall induced by the development of convective cells in a frontal zone inside a Mediterranean cyclone (Berezhnaya et al., 2019). Total amount of precipitation on 24–25 October varied from 253 to 362 mm in the Tuapse River basin and 208.9 mm in the Shakhe River basin to 53.2 mm near the Sochi River mouth and 83.6–112 mm in the Mzymta River basin.

Combination of two mechanisms, namely, heavy precipitation influenced by mountainous relief and rapid concentration of river runoff from steep mountain slopes in the river basins, resulted in formation of flash floods at the considered rivers (Marchi et al., 2010; Borga et al., 2011; Kuksina et al., 2017). Peak discharges at these rivers varied from 127 to 706 m^3/s (Fig. 3), which is 1–2 orders of magnitude greater than their mean annual discharge rates. The return period of the observed flood based on 40–82 years of gauge observations is equal to 50 years for the Mzymta River, 10–20 years for the Khosta and Dagomys rivers, 2–4 years for Kudepsta, Matsesta, Sochi, Shakhe, and Psezuapse rivers. The extremely intense runoff formation was accompanied by severe erosion at the river catchments and stream channels, which resulted in increased runoff of terrigenous sediments (Borga et al., 2014).

Sediment transport in the upper parts of the river catchments within one extreme flooding event can be close to the average annual estimates of the erosion rate (Tsyplenkov et al., 2017; Ivanova et al., 2018). During the flooding event on 25 June 2015, similar to the studied one, almost 90% of the average annual volume of suspended sediment was discharged from the Khosta River. During the flooding event of 23–28 October 2018 the Khosta River delivered to the sea approximately 80% of its average annual sediment yield, while the related share of the Mzymta River was approximately 40% (https://gmvo.skniivh.ru/). Similarly to the abrupt increase of suspended sediment discharge during flash floods, FML discharge from the considered small rivers is believed to significantly increase, as compared to average climatic discharge conditions. Flooding of coastal urbanized areas in the lower parts of the rivers (Albano et al., 2016), which is typical for the study area (Alexeevsky et al., 2016), accompanies intense litter removal from the rural settlements.

We performed simulation of spreading of the river plumes, as well as the delivery and fate of river-borne floating particles shortly before, during, and after the large flooding event which occurred in the end of October 2018 in the study area. The simulation by the Lagrangian particle model covered the period during (24–25 October 2018) and after (26 October–4 November 2018) this flooding event. Wind forcing during the simulation period was highly variable, it switched twice

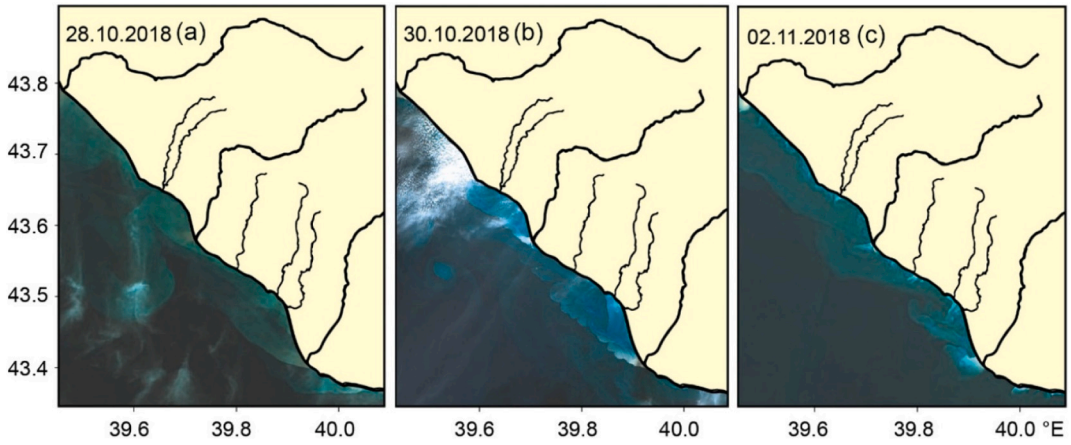

Fig. 2. Sentinel-2 optical satellite images of the study area demonstrating the considered river plumes on 28 October (a), 30 October (b), and 2 November (c).

between downwelling-favorable on 24 October and 26–28 October and upwelling-favorable on 25–26 October and 28 October–4 November (Fig. 4, bottom). Daily averaged values of wind speed at the study area varied between 1 and 6.5 m/s, while their mean value was 2.5 m/s. The top panel in Fig. 4 shows that the Stokes drift reached maximal values of 0.3 m/s during the peak of the flooding event (at night of 24–25 October) during a strong downwelling-favorable southeasterly wind. The second peak of the Stokes drift (up to 0.1 m/s) was observed on 27 October also during the prevailing southeasterly winds.

On 25 October (Supplementary material – 1. Fig. 2), i.e., 3 h after the flood peak (Fig. 3), the numerical model reproduced the development of the river plume bulges (Yankovsky and Chapman, 1997) characterized by anticyclonic vorticity, low salinity, and increased horizontal gradients of density. The northwestward alongshore flow was slightly shifted offshore due to formation of the river bulges. Well-developed convergence zones were formed at the fronts between the river plumes and the ambient saline sea waters. On 26 October (Supplementary material – 1. Fig. 3) the upwelling-favorable northwesterly wind significantly modified the plume spreading patterns. The Ekman transport directed towards the open sea pressed the northwestward current farther from the coast. The freshened coastal stripe formed as a result of coalescence of multiple river plumes widened approximately twice, as compared to that of the day before. The weak water flow in the southeastward direction and the weak anticyclonic vortices were observed near the coast.

Change of wind forcing to downwelling-favorable during the period from 26 to 28 October resulted in a situation when all three factors, namely, the general circulation of the Black Sea (the Rim Current), the wind-driven coastal flow, and the coastal buoyant jet controlled by river discharge, contributed to the northwestward transport in the coastal area. As a result, the velocity of the alongshore northwestward current increased up to 0.4–0.5 m/s and the current itself moved close to the shore, which was observed on 28 October (Supplementary material – 1. Fig. 4). Then the wind changed to upwelling-favorable and on 30–31 October, i.e. 4–5 days after the flood, and the freshened stripe dissipated. As a result, the northwestward flow again shifted towards the open sea and the river plumes returned to their average state as was observed before the flood (Supplementary material – 1. Figs. 5–6).

In order to study the influence of the Stokes drift on FML transport during the flooding event we calculated trajectories of the Lagrangian floating particles with and without the Stokes drift (Figs. 5–6). The main difference between the reconstructed spreading patterns of the Lagrangian particles consists in shift of the particles towards the shoreline in presence of the Stokes drift. Trajectories of the particles originated from the Mzymta River, the largest river in the region, were less affected by the Stokes drift due to larger outflow velocities and larger bulge, as compared to the other considered rivers. For both cases the particles originated from different river mouths distinctly aggregated in a single convergence line (Fig. 6e, Fig. 7e).

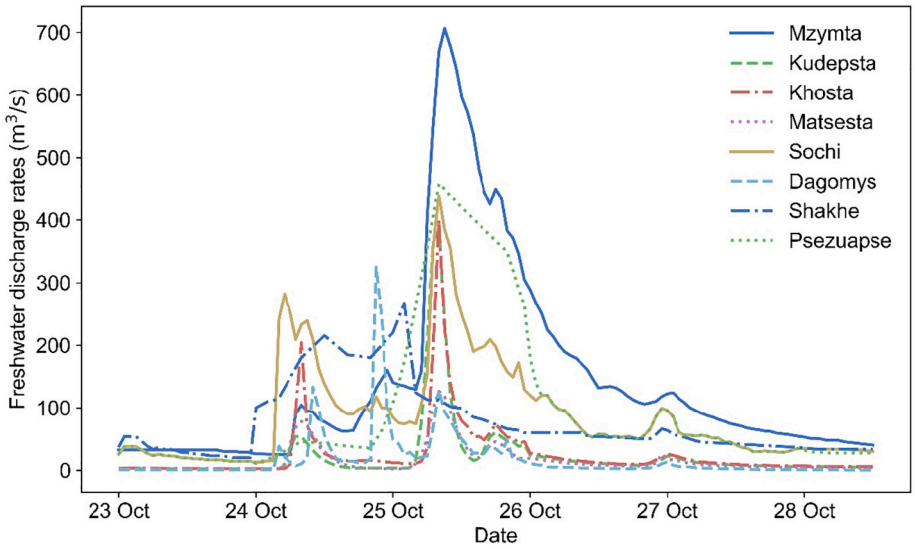

Fig. 3. Freshwater discharge rates of the Mzymta, Kudepsta, Khosta, Matsesta, Sochi, Dagomys, Shakhe and Psezuapse rivers during 23–28 October 2018.

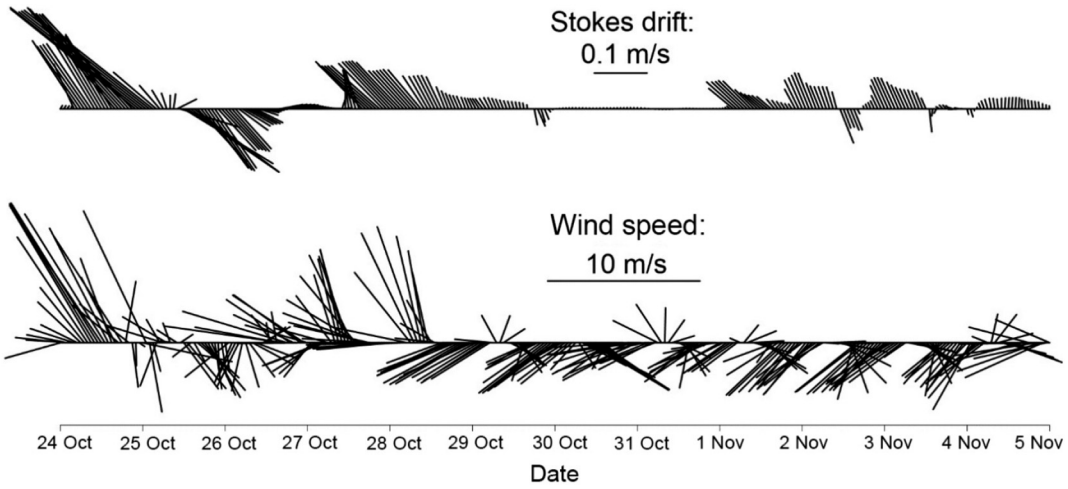

Fig. 4. The 10-m level wind speed (bottom) and the Stokes drift (top) time series at the characteristic sea point on the model beam corresponding to the Sochi River during the period 24 October–4 November 2018.

4. Discussion

4.1. FML accumulation areas at the sea

The obtained results showed that during and shortly after the flood the particles which originated from different river mouths steadily moved in the northwestward direction even with the disturbing Stokes drift effect (Fig. 6). As a result of advection the tracks of the particles discharged from the different rivers merged together and most of the particles were trapped within a narrow line. This line is associated with a sharp salinity gradient and is characterized by negative divergence values (Supplementary material – 1. Fig. 6). The width of this convergence line obtained by the Lagrangian particle model is equal to 3 m. This result is supported by aerial images of the river plumes in the study area taken by a quadcopter. These images show that peak concentrations of FML at the coastal sea are distinctly located at the fronts

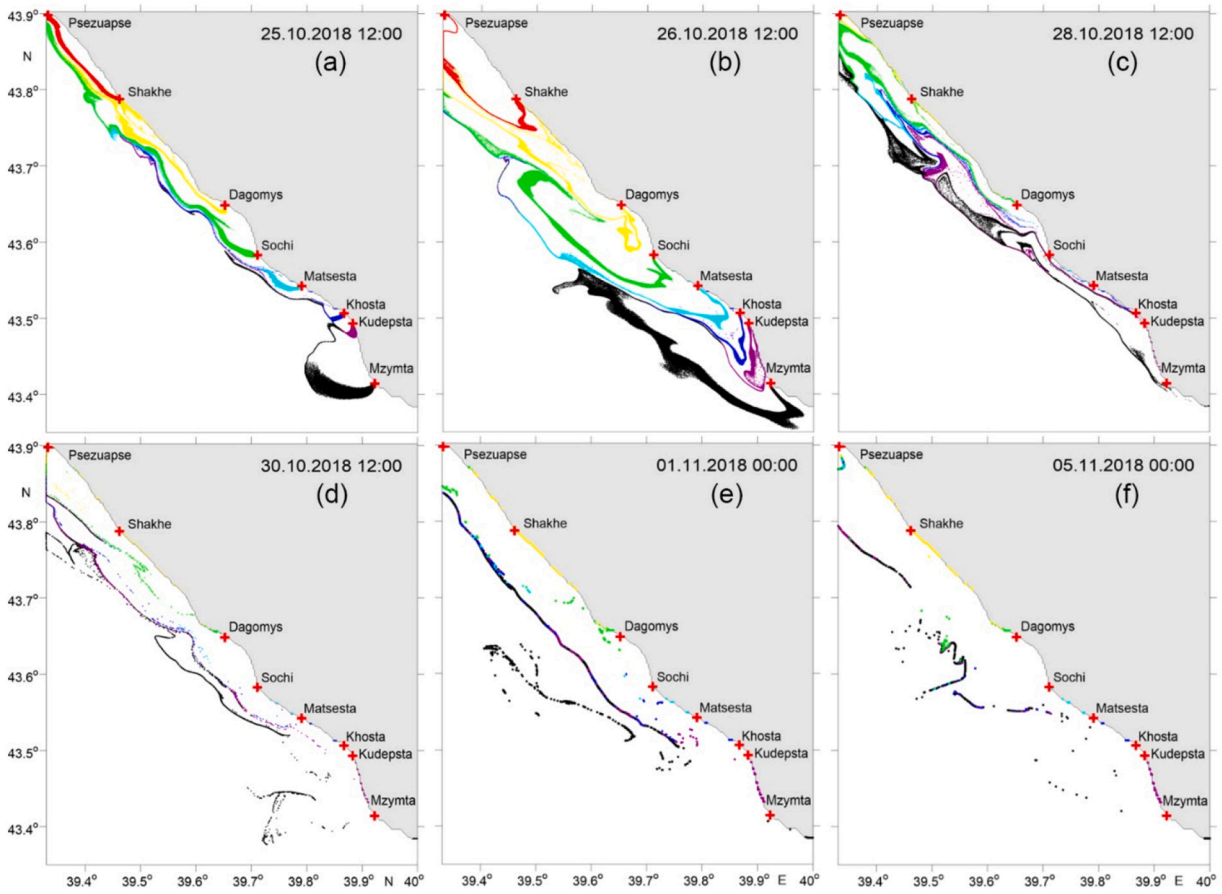

Fig. 5. The simulated distribution of the Lagrangian floating particles (without the Stokes drift) seeded in river mouths in proportion to the actual river discharge rate during the flooding period on 25 October (a), 26 October (b), 28 October (c), 30 October (d), 1 November (e), and 5 November (f) at 12:00 UTC. The particles originated from different rivers are marked by different colors.

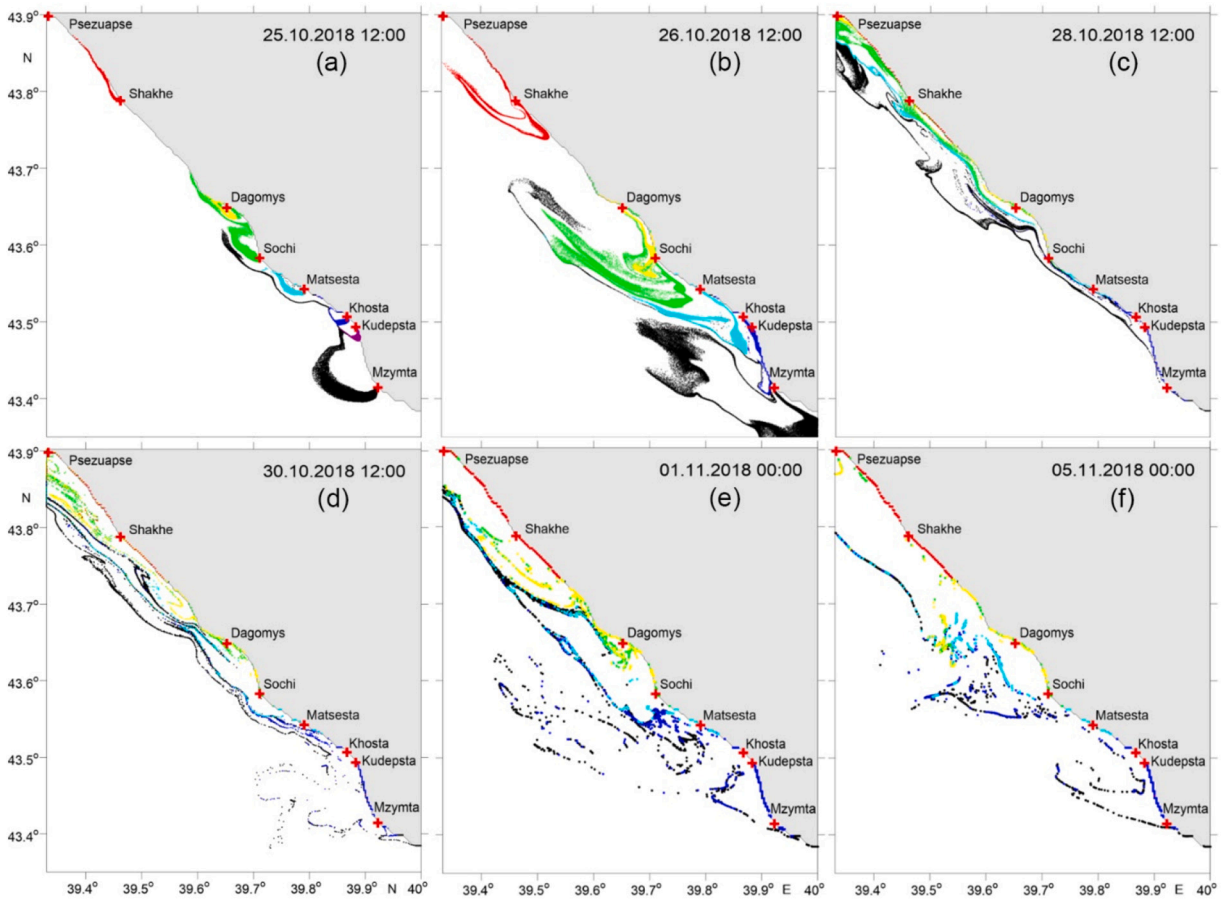

Fig. 6. Same as in Fig. 5, but with the Stokes drift.

between the river plumes and the ambient sea (Fig. 7). These marine litter patches are several meters wide; they are irregularly distributed along the plume front, which is also consistent with the modelling results. Aerial observations showed that FML patches are stable during at least several hours of observations and move with the border of a river plume.

Accumulation of floating particles in convergence zones was reported in many previous studies (Maximenko et al., 2012; Cózar et al., 2015; Stanev and Ricker, 2019; Van Sebille et al., 2020). In this study we expand the conclusion that river-borne FML is concentrated at the convergence zones associated with horizontal salinity gradients, i.e., river plume borders. We show that the presence of the convergence area is not enough to accumulate FML in case of an unsteady velocity field with alternating divergence, which is the case of river plumes (Supplementary material – 2, Eqs. (1)–(2)). Based on strictly defined mathematical notions, we reveal that the aggregation of floating particles on a frontal line (convergence line) occurs only in presence of a stagnation point.

The width of this convergence line described above can be underestimated since the particle trajectories were calculated without taking into account random displacements caused by the subgrid diffusion. The upper bound of this width is equal to ~50 m (Supplementary material – 2).

Aerial surveys on marine litter performed within the scope of local monitoring programs during 2004–2005 (BSC, 2007, 2019) showed that the major quantity of FML inflows to the Russian Black Sea during

Fig. 7. Aerial images of the sharp front between turbid river plume and ambient sea illustrating accumulation of FML at the convergence zone at this front.

spring-summer freshet and is positively correlated with the river discharge rate. The largest concentrations of FML in the sea were registered at the 5–25 km wide coastal zone. These results support our findings that, first, short-term flash floods at small rivers are important sources of FML in the study area at least on synoptic time scale and, second, that despite the fact that river-borne FML is transported far off river mouths, it remains arrested near the coast within the coalesced river plumes.

4.2. FML accumulation areas at the shoreline

Large volumes of FML are washed ashore from sea and accumulate at shorelines (Barnes et al., 2009; Galgani et al., 2015). In order to detect the related accumulation areas of FML at the shoreline of the study area, we simulated and detected the particles washed ashore during the study period. A particle is considered to be trapped at the shoreline, if it was advected to a model sea bin adjacent to a land bin. The comparison of the modelling results with and without the Stokes drift demonstrated its role in washing ashore of FML. We found that without the Stokes drift only 3.6% of the total number of the released particles were washed ashore within the study region from 24 October to 1 November 2018 (Table 1). In presence of the Stokes drift the number of washed ashore particles increased by one order of magnitude to 46.0%. In presence of the Stokes drift the trapped particles are more uniformly distributed along the shoreline, because the Stokes drift velocity field is more uniform than the current velocity field in presence of sub-mesoscale eddies (Fig. 8). As a result, the Stokes drift induced by surface waves provides significantly greater contribution to coastal pollution by FML, as compared to coastal currents.

In order to study the role of coastal currents in formation of FML accumulation zones at the shoreline, we performed the detailed analysis of the trajectories of the trapped particles for the model run without the Stokes drift (Fig. 8a). The majority of particles were trapped during the flooding event (24–25 October) and three days after (26–28 October). Initial accumulation areas of washed ashore particles appeared at the shoreline segments located southeastward from the Kudepsta and Shakhe rivers (Fig. 8a, accumulation areas 2, 6) that were formed mainly by particles discharged from the Dagomys and Kudepsta rivers. As it was mentioned before, the northwestward alongshore flow was shifted offshore due to the formation of the river bulges, however, the secondary flooding peaks caused accumulation of particles near local shoreline irregularities (Elkin and Zatsepin, 2013; Zhurbas et al., 2017). Coastal accumulation of particles continued on 25–26 October during upwelling-favorable wind forcing. Northwestern current moved off the coast and particles were advected in the southeastern direction (Fig. 5a) resulting in intense washing ashore southeastward from the Kudepsta and Shakhe river mouths (Fig. 8a, accumulation areas 2, 6).

The major particle discharge occurred during the period from 26 to 28 October during downwelling-favorable wind, when the alongshore current became stronger and was pressed towards the shore (Fig. 5b). New accumulation areas of particles appeared at several segments of the shoreline, namely, between the mouths of the Khosta and Matsesta rivers (Fig. 8a, accumulation area 5) dominated by particles discharged from the Khosta River; between the mouths of the Matsesta and Sochi rivers (Fig. 8a, accumulation areas 4) dominated by particles discharged from the Matsesta, Sochi and Khosta rivers; near the Dagomys river mouth (Fig. 8a, accumulation area 3) dominated by particles discharged from the Sochi and Dagomys rivers; between the mouths of the Dagomys and Shakhe rivers (Fig. 8a, accumulation area 2) dominated by particles discharged from the Sochi and Dagomys rivers, and between the mouths of the Shakhe and Psezuapse rivers (Fig. 8a, accumulation area 1) dominated by particles discharged from the Sochi, Dagomys and Shakhe rivers. However, particles discharged from the Mzymta River, the largest river in the study area, were not intensely washed ashore and remained in the sea. This feature is presumably caused by large size of the Mzymta plume and more intense advection of the related particles off the river mouth to the open sea.

To get quantitative estimate of the net effect of river plume dynamics during the flood on FML transport and shoreline contamination, we performed additional numerical experiment with “no flood” discharge conditions. Average climatic river discharge formed relatively small river plumes. As a result, the number of particles trapped at the shoreline within the study region from 24 October to 1 November 2018 significantly increased to 5.3% and 57.9% for the model runs without and with the Stokes drift.

Note that Table 1 contains estimates of $N_{onshore}$, N_{onsea} and N_{out} calculated for the “basic” modelling period from 24 October to 1 November 2018 and an extended period from 24 October to 5 November 2018 to show that the extension of modelling period does not cause any considerable changes in these estimates.

Table 1
The fate of floating particles for different numerical experiments. N_{total} is the total number of released floating particles, $N_{onshore}$ is the number of particles washed ashore within the study region, N_{onsea} is the number of particles remaining in the sea within the study region; $N_{out} = N_{total} - N_{onsea} - N_{onshore}$ is the number of particles advected off the study region.

	N_{total}	N_{out}	N_{onsea}	$N_{onshore}$
01.11.2018 00:00 UTC	372,690	353,782	5735	13,384
No Stokes drift	100%	94.9%	1.5%	3.6%
Actual river discharge				
01.11.2018 00:00 UTC	372,690	349,876	3150	19,664
No Stokes drift	100%	93.9%	0.8%	5.3%
Climate river discharge				
01.11.2018 00:00 UTC	372,690	186,955	14,250	171,485
Stokes drift included	100%	50.2%	3.8%	46.0%
Actual river discharge				
01.11.2018 00:00 UTC	372,690	141,304	15,710	215,675
Stokes drift included	100%	37.9%	4.2%	57.9%
Climate river discharge				
05.11.2018 00:00 UTC	372,690	358,663	3113	10,914
No Stokes drift	100%	96.2%	0.8%	2.9%
Actual river discharge				
05.11.2018 00:00 UTC	372,690	308,248	45,671	18,771
No Stokes drift	100%	82.7	12.3%	5.0%
Climate river discharge				
05.11.2018 00:00 UTC	372,690	189,942	13,065	169,683
Stokes drift included	100%	51.0%	3.5%	45.5%
Actual river discharge				
05.11.2018 00:00 UTC	372,690	142,778	18,074	211,838
Stokes drift included	100%	38.3%	4.9%	56.8%
Climate river discharge				

5. Summary and conclusions

This study is focused on delivery and fate of floating marine litter (FML), which is carried by rivers to the coastal sea. River-borne FML is transported by buoyant river plumes off river mouths to the open sea, while a certain share of river-borne FML is washed ashore contaminating the shoreline. Using a combination of the Eulerian INMOM model and the Lagrangian particle model we reconstructed the fate of river-borne FML during a large flooding event, which occurred in the northeastern part of the Black Sea in October 2018. INMOM model with a non-uniform horizontal grid was applied to reproduce the general Black Sea circulation with an increased spatial resolution in the study area (~200 m). The reconstructed current velocities in the uppermost model layer and the Stokes drift velocities data were applied for the Lagrangian particle model that simulated spreading in the coastal sea and washing ashore of floating particles. The river discharge data were reconstructed with high temporal resolution using an event-based rainfall-runoff KW-GIUH model, which is essential for accurate simulation of the flooding event. Based on the obtained simulation results, we analyzed the influence of the short-term flooding event on spreading of river-borne FML and its accumulation in the sea and at the shoreline.

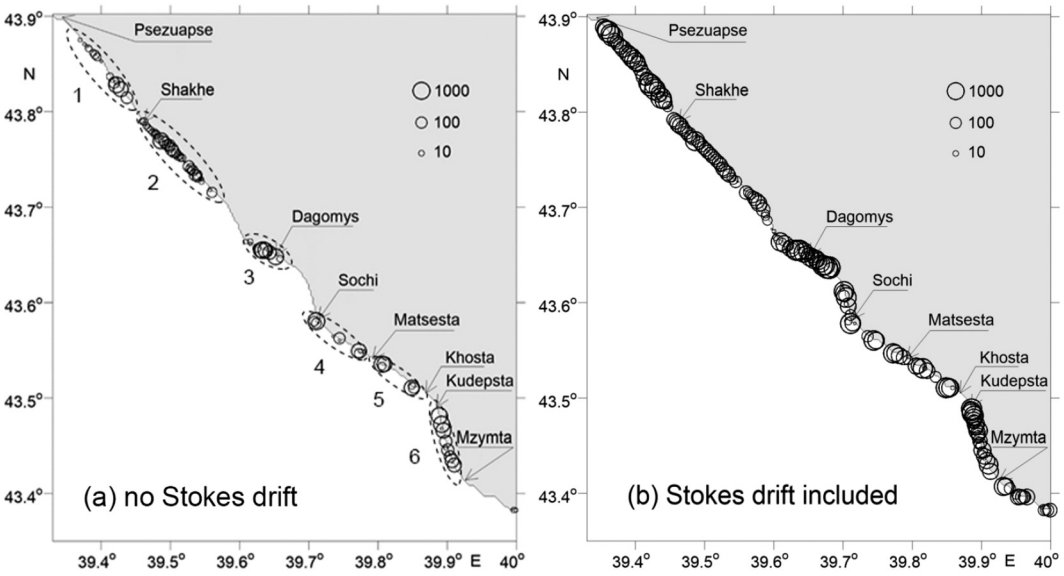

Fig. 8. Distribution of floating particles trapped at the shoreline without (a) and with (b) the Stokes drift. The particle concentration (the number of particles per 250 m × 250 m bin) is shown by circles of different size, the radius of the circle is proportional to the decimal logarithm of the concentration. The numbers 1–6 indicate the main accumulation areas of particles at the shoreline.

The numerical simulation showed rapid increase of areas of river plumes followed by their coalescence as a result of heavy rainfall at the northeastern coast of the Black Sea. Distinct zones of convergence of surface flow were formed at the sharp frontal zoned between the freshened river plumes and the ambient saline sea water. The majority of river-borne FML were accumulated at these convergence zones within the individual plumes, where the horizontal divergence of current velocity is negative and the cross-zone velocity component is alternating. These zones have relatively small areas, therefore, accurate reconstruction of delivery and fate of river-borne litter in the sea requires numerical modelling with high spatial resolution. On the other hand, the transport of FML from the plumes to the saline sea and between the plumes was negligible. The coalescence of multiple river plumes that occurred shortly after the main flood peak resulted in formation of a narrow stripe of surface flow between the buoyant river plumes and saline sea water. As a result, the convergence areas at the frontal zones of the individual river plumes merged into one narrow convergence line (~3 m wide) stretched along the shoreline on a distance of 6–8 km from the shoreline.

FML discharged from different rivers of the study area accumulated at this single convergence line and then was transported along this line in the northwestward direction. As a result, FML was quickly removed far off the river mouths and mixed to almost homogeneous state, i.e., FML originating from closely located rivers had similar concentrations at long segments of the convergence line. The northwestward transport of FML along the convergence line continued until the dissipation of the freshened stripe as a result of mixing between the merged river plumes and the ambient sea. After that FML was released to the saline sea and its spreading was governed by coastal circulation.

During and several days after the flooding event approximately half of river-borne FML was washed ashore and accumulated at the shoreline mainly due to the Stokes drift. Without the Stokes drift coastal trapped FML had non-uniform distribution along the coast. Its accumulation areas can be classified into two types, namely, typical and “uncommon”. Typical accumulation areas that are expected to form after every local flooding event are located downstream the river mouths (due to direction of the Coriolis force) and are determined by the river discharge rate, the semi-geostrophic alongshore northwestward current, and the sub-mesoscale anticyclonic/cyclonic eddies formed behind the local shoreline features (headlands). Formation of the “uncommon” accumulation areas is governed by direction of prevailing winds and is prone to large inter-event variability due to variability of wind forcing. In presence of the Stokes drift the discharged particles were more uniformly distributed along the shoreline. Comparison of numerical simulation with flooding and non-flooding river discharge conditions showed that dynamics and interaction of small river plumes contribute substantially to transport of FML. They provided noticeable decrease of local contamination of the shoreline and the respective increase of litter dispersion in the coastal sea.

The majority of marine litter is estimated to originate from land-based sources and rivers which are responsible for up to 80% of the plastic floating litter in the sea (Allsopp et al., 2006; Coyle et al., 2020). Considering such a significant contribution, several previous studies were devoted to the role of rivers in marine plastic pollution of coastal sea areas. These studies were mostly focused on large and heavily polluted rivers, which provide predominant volume of the riverine plastic pollution on a regional scale (Fok and Cheung, 2015; Veerasingam et al., 2016). In particular, among the numerous rivers, which drain the Black Sea, only the influence of the largest Danube River on marine plastic distribution was studied and estimated (Lechner et al., 2014). According to the recent research of Stanev and Ricker (2019), due to the dominant northerly winds and the resulting Ekman and Stokes drift, concentrations of river-borne FML in the north-western and western parts of the Black Sea are significantly higher than in the rest of the sea. Moreover, the influence of the non-local Danube and Dnieper rivers on the distribution of FML in the north-eastern part of the Black Sea is very small in comparison with the influence of small local rivers. The volumes of suspended sediments and FML share that assumed to be similar to the suspended sediments share during flooding events can be up to 30–80% of the respective annual volumes (Ivanova et al., 2018) making the difference between the contribution values of pollution from large and small rivers even more substantial.

This result demonstrates that the influence of small rivers on local pollution in the coastal area during flooding events is significant due to the fact that river-borne FML discharged from small rivers is concentrated in their plumes and does not spread over a large area as compared to the FML discharge from the Danube and Dnieper rivers. This effect is short-term (several weeks a year), but during this time a large amount of river-borne FML is accumulated in the coastal sea area and then is partly washed ashore. As a result, the cumulative role of small rivers in the delivery and fate of floating marine plastic can be of the same importance as that of the large rivers at least for certain

regions and certain time periods. Thus, the ongoing pollution monitoring, reducing, and mitigation programs can be significantly improved by considering the delivery and fate of plastic pollution from small rivers during flooding periods. The related detailed assessment of the role of small rivers on pollution at coastal sea areas and shoreline is within the scope of future work.

CRediT authorship contribution statement

Evgeniya Korshenko: Methodology, Software, Validation, Formal analysis, Investigation, Resources, Writing - original draft, Writing - review & editing, Visualization. **Victor Zhurbas:** Conceptualization, Methodology, Software, Validation, Formal analysis, Investigation, Resources, Writing - original draft, Writing - review & editing, Visualization. **Alexander Osadchiev:** Conceptualization, Methodology, Validation, Formal analysis, Investigation, Resources, Writing - original draft, Writing - review & editing, Supervision. **Pelagiya Belyakova:** Methodology, Software, Validation, Formal analysis, Investigation, Resources, Writing - original draft.

Declaration of competing interest

The authors declare that they have no known competing financial interests or personal relationships that could have appeared to influence the work reported in this paper.

Acknowledgements

The authors are grateful to many colleagues from Zubov State Oceanographic Institute for valuable support and wish to thank Nikolay Diansky, Vladimir Fomin, and Irina Panasenkova. This research was funded by the Ministry of Science and Higher Education of the Russian Federation, theme 0149-2019-0003 (numerical modelling of sea circulation); by the Russian Science Foundation, research project 17-77-30006 (processing of river discharge data, flash flood simulation) and research project 18-17-00156 (study of spreading and dynamics of river plumes); by the Russian Foundation for Basic Research, research project 19-45-233007 (data processing from an Automated Flood Monitoring System of the Krasnodar Territory) and research project 19-55-80004 (study of fate of the floating plastic litter).

Appendix A. Supplementary data

Supplementary data to this article can be found online at https://doi.org/10.1016/j.marpolbul.2020.111678.

References

Albano, R., Sole, A., Mirauda, D., Adamowski, J., 2016. Modelling large floating bodies in urban area flash-floods via a Smoothed Particle Hydrodynamics model. J. Hydrol. 541, 344–358. https://doi.org/10.1016/j.jhydrol.2016.02.009.

Alexeevsky, N.I., Magritsky, D.V., Koltermann, K.P., Krylenko, I.N., Toropov, P.A., 2016. Causes and systematics of inundations of the Krasnodar territory on the Russian Black Sea coast. Nat. Hazards Earth Syst. Sci. 16, 1289–1308. https://doi.org/10.5194/nhess-16-1289-2016.

Allsopp, M., Walters, A., Santillo, D., Johnston, P., 2006. Plastic Debris in the World's Oceans. Greenpeace, Amsterdam, The Netherlands.

Atwood, E.C., Falcieri, F.M., Piehl, S., Bochow, M., Matthies, M., Franke, J., Carniel, S., Sclavo, M., Laforsch, C., Siegert, F., 2019. Coastal accumulation of microplastic particles emitted from the Po River, Northern Italy: comparing remote sensing and hydrodynamic modelling with in situ sample collections. Mar. Pollut. Bull. 138, 561–574. https://doi.org/10.1016/j.marpolbul.2018.11.045.

Avio, C.G., Gorbi, S., Milan, M., Benedetti, M., Fattorini, D., D'Errico, G., Pauletto, M., Bargelloni, L., Regoli, F., 2015. Pollutants bioavailability and toxicological risk from microplastics to marine mussels. Environ. Pollut. 198, 211–222. https://doi.org/10.1016/j.envpol.2014.12.021.

Avio, C.G., Gorbi, S., Regoli, F., 2017. Plastics and microplastics in the oceans: from emerging pollutants to emerged threat. Mar. Environ. Res. 128, 2–11. https://doi.org/10.1016/j.marenvres.2016.05.012.

Bagaev, A., Khatmullina, L., Chubarenko, I., 2018. Anthropogenic microlitter in the Baltic Sea water column. Mar. Pollut. Bull. 129 (2), 918–923. https://doi.org/10.1016/j.marpolbul.2017.10.049.

Balabanov, I.P., Nikiforov, S.P., Pashkovskiy, I.S., 2011. Imeretinskaya lowland. In: Natural Geological Conditions, Problems of Development. Nedra Publishing Co, Moscow (in Russian).

Barnes, D.K.A., 2002. Invasions by marine life on plastic debris. Nature 416, 808–809. https://doi.org/10.1038/416808a.

Barnes, D.K.A., Galgani, F., Thompson, R.C., Barlaz, M., 2009. Accumulation and fragmentation of plastic debris in global environments. Philosophical Transactions of the Royal Society of London – B. Biological Sciences 364, 1985–1998. https://doi.org/10.1098/rstb.2008.0205.

Bat, L., Öztekin, A., Arıcı, E., 2017. Marine Litter Pollution in the Black Sea: Assessment of the Current Situation in Light of the Marine Strategy Framework Directive in Black Sea Marine Environment: The Turkish Shelf. Turkish Marine Research Foundation, Istanbul.

Berezhnaya, T.V., Golubev, A.D., Parshina, L.N., 2019. Anomalous hydrometeorological phenomena on the Russian Federation Territory in October 2019. Russ. Meteorol. Hydrol. 1 (in Russian).

Borga, M., Anagnostou, E.N., Bloeschl, G., Creutin, J.-D., 2011. Flash flood forecasting, warning and risk management: the HYDRATE project. Environ. Sci. Pol. 834–844. https://doi.org/10.1016/j.envsci.2011.05.017.

Borga, M., Stoffel, M., Marchi, L., Marra, F., Jakob, M., 2014. Hydrogeomorphic response to extreme rainfall in headwater systems: flash floods and debris flows. J. Hydrol. 518, 194–205. https://doi.org/10.1016/j.jhydrol.2014.05.022.

Bruge, A., Barreau, C., Carlot, J., Collin, H., Moreno, C., Maison, P., 2018. Monitoring litter inputs from the Adour River (Southwest France) to the marine environment. Journal of Marine Science and Engineering 6 (1), 24. https://doi.org/10.3390/jmse6010024.

BSC [Black Sea Commission], 2007. Marine Litter in the Black Sea Region: A Review of the Problem. Black Sea.

BSC [Black Sea Commission], 2019. State of the Environment of the Black Sea (2009–2014/5). Publications of the Commission on the Protection of the Black Sea Against Pollution, Istanbul, Turkey. (811 pp.).

Cheung, P.K., Cheung, L.T.O., Fok, L., 2016. Seasonal variation in the abundance of marine plastic debris in the estuary of a subtropical macro-scale drainage basin in South China. Sci. Total Environ. 562, 658–665. https://doi.org/10.1016/j.scitotenv.2016.04.048.

Chubarenko, I., Efimova, I., Bagaeva, M., Bagaev, A., Isachenko, I., 2020. On mechanical fragmentation of single-use plastics in the sea swash zonewith different types of bottom sediments: insights from laboratory experiments. Mar. Pollut. Bull. 150, 110726. https://doi.org/10.1016/j.marpolbul.2019.110726.

Courtene-Jones, W., Quinn, B., Gary, S.F., Mogg, A.O.M., Narayanaswamy, B.E., 2017. Microplastic pollution identified in deep-sea water and ingested by benthic invertebrates in the Rockall Trough, North Atlantic Ocean. Environ. Pollut. 231, 271–280. https://doi.org/10.1016/j.envpol.2017.08.026.

Coyle, R., Hardiman, G., O'Driscoll, K., 2020. Microplastics in the marine environment: a review of their sources, distribution processes and uptake into ecosystems. Case Studies in Chemical and Environmental Engineering. https://doi.org/10.1016/j.cscee.2020.100010.

Cózar, A., Sanz-Martín, M., Martí, E., González-Gordillo, J.I., Ubeda, B., Gálvez, J.Á., Irigoien, X., Duarte, C.M., 2015. Plastic accumulation in the Mediterranean Sea. PLoS One 10 (4), e0121762. https://doi.org/10.1371/journal.pone.0121762.

Cózar, A., Martí, E., Duarte, C.M., García-de-lomas, J., Van Sebille, E., Ballatore, T.J., Eguiluz, V.M., Gonzalez-Gordillo, J.I., Pedrotti, M.L., Echevarria, F., Toruble, R., Irigoien, X., 2017. The Arctic Ocean as a dead end for floating plastics in the North Atlantic branch of The Thermohaline Circulation. Sci. Adv. 3, 1–8. https://doi.org/10.1126/sciadv.1600582.

Derraik, J.G., 2002. The pollution of the marine environment by plastic debris: a review. Mar. Pollut. Bull. 44, 842–852. https://doi.org/10.1016/S0025-326X(02)00220-5.

Diansky, N.A., Fomin, V.V., Zhokhova, N.V., Korshenko, A.N., 2013. Simulations of currents and pollution transport in the coastal waters of Big Sochi. Izvestiya, Atmospheric and Oceanic Physics 49, 611–621. https://doi.org/10.1134/s0001433813060042.

Eerkes-Medrano, D., Thompson, R.C., Aldridge, D.C., 2015. Microplastics in freshwater systems: a review of the emerging threats, identification of knowledge gaps and prioritisation of research needs. Water Res. 75, 63–82. https://doi.org/10.1016/j.watres.2015.02.012.

Elkin, D.N., Zatsepin, A.G., 2013. Laboratory investigation of the mechanism of the periodic eddy formation behind capes in a coastal sea. Oceanology 53, 24–35. https://doi.org/10.1134/S0001437012050062.

Eriksen, M., Laurent, C.M.L., Henry, S.C., Thiel, M., Moore, C.J., Borerro, J.C., Galgani, F., Ryan, P.G., Reisser, J., 2014. Plastic pollution in the world's oceans: more than 5 trillion plastic pieces weighing over 250,000 tons afloat at sea. PLoS One 9 (12), e111913. https://doi.org/10.1371/journal.pone.0111913.

Fok, L., Cheung, P.K., 2015. Hong Kong at the Pearl River Estuary: a hotspot of microplastic pollution. Mar. Pollut. Bull. 99, 112–118. https://doi.org/10.1016/j.marpolbul.2015.07.050.

Galgani, F., Hanke, G., Maes, T., 2015. Global distribution, composition and abundance of marine litter. In: Bergmann, M., Gutow, L., Klages, M. (Eds.), Marine Anthropogenic Litter. Springer, Cham. https://doi.org/10.1007/978-3-319-16510-3_2.

Geyer, R., Jambeck, J.R., Law, K.L., 2017. Production, use, and fate of all plastics ever made. Sci. Adv. 3 (7), e1700782.

Gonchukov, L.V., Bugaets, A.N., Gartsman, B.I., Lee, K.T., 2019. Weather radar data for hydrological modelling: an application for south of Primorye region. Water Resources 46 (2), S25–S30. https://doi.org/10.1134/S0097807819080098.

Gregory, M.R., 2009. Environmental implications of plastic debris in marine settings – entanglement, ingestion, smothering, hangers-on, hitch-hiking and alien invasions.

Philosophical Transactions of the Royal Society of London – B. Biological Sciences 364, 2013–2025. https://doi.org/10.1098/rstb.2008.0265.
Hirai, H., Takada, H., Ogata, Y., Yamashita, R., Mizukawa, K., Saha, M., Kwan, C., Moore, C., Gray, H., Laursen, D., Zettler, E.R., Farrington, J.W., Reddy, C.M., Peacock, E.E., Ward, M.W., 2011. Organic micropollutants in marine plastics debris from the open ocean and remote and urban beaches. Mar. Pollut. Bull. 62, 1683–1692. https://doi.org/10.1016/j.marpolbul.2011.06.004.
Horner-Devine, A.R., Hetland, R.D., MacDonald, D.G., 2015. Mixing and transport in coastal river plumes. Annu. Rev. Fluid Mech. 47 (1), 569–594. https://doi.org/10.1146/annurev-fluid-010313-141408.
Horton, A.A., Svendsen, C., Williams, R.J., Spurgeon, D.J., Lahive, E., 2017. Large microplastic particles in sediments of tributaries of the River Thames, UK–abundance, sources and methods for effective quantification. Mar. Pollut. Bull. 114, 218–226. https://doi.org/10.1016/j.marpolbul.2016.09.004.
Ivanova, N.N., Golosov, V.N., Tsyplenkov, A.S., Kuznetsova, Yu.S., Botavin, D.V., 2018. Sources of the basin component of the sediment yield on the small river in the foothill-lowland zone of the Black Sea coast of the Caucasus (using the example of the Tsanyk River). Engineering Survey XII (7–8), 62–74. https://doi.org/10.25296/1997-8650-2018-12-7-8-62-74.
Jaoshvili, S., 2002. The rivers of the Black Sea. European Environmental Agency, Technical Report No. 71.
Korotkina, O.A., Zavialov, P.O., Osadchiev, A.A., 2011. Submesoscale variability of the current and wind fields in the coastal region of Sochi. Oceanology 51, 745–754. https://doi.org/10.1134/s0001437011050109.
Korotkina, O.A., Zavialov, P.O., Osadchiev, A.A., 2014. Synoptic variability of currents in the coastal waters of Sochi. Oceanology 54, 545–556. https://doi.org/10.1134/s0001437014040079.
Kuksina, L.V., Golosov, V.N., Kuznetsova, Yu.S., 2017. Cloudburst floods in mountains: state of knowledge, occurrence, factors of formation. Geogr. Nat. Resour. 38, 20–29. https://doi.org/10.1134/S1875372817010036.
La Beur, L., Henry, L.-A., Kazanidis, G., Hennige, S., McDonald, A., Shaver, M., Roberts, M.J., 2019. Baseline assessment of marine litter and microplastic ingestion by cold-water coral reef benthos at the East Mingulay Marine Protected Area (Sea of the Hebrides, western Scotland). Front. Mar. Sci. https://doi.org/10.3389/fmars.2019.00080.
Law, K.L., Morét-Ferguson, S.E., Maximenko, N.A., Proskurowski, G., Peacock, E.E., Hafner, J., Reddy, C.M., 2010. Plastic accumulation in the North Atlantic Subtropical Gyre. Science 329, 1185–1188. https://doi.org/10.1126/science.1192321.
Law, K.L., Morét-Ferguson, S.E., Goodwin, D.S., Zettler, E.R., DeForce, E., Kukulka, T., Proskurowski, G., 2014. Distribution of surface plastic debris in the Eastern Pacific Ocean from an 11-year data set. Environmental Science & Technology 48, 4732–4738. https://doi.org/10.1021/es4053076.
Lebreton, L.C.M., van der Zwet, J., Damsteeg, J.-W., Slat, B., Andrady, A., Reisser, J., 2017. River plastic emissions to the world's oceans. Nat. Commun. 8, 15611. https://doi.org/10.1038/ncomms15611.
Lebreton, L., Egger, M., Slat, B., 2019. A global mass budget for positively buoyant macroplastic debris in the ocean. Sci. Rep. 9, 12922. https://doi.org/10.1038/s41598-019-49413-5.
Lechner, A., Keckeis, H., Lamesberger-Loisl, F., Zens, B., Krusch, R., Tritthart, M., Glas, M., Schludermann, E., 2014. The Danube so colourful: a potpourii of plastic litter outnumbers fish larvae in Europe's second largest river. Environ. Pollut. 188, 177–181. https://doi.org/10.1016/j.envpol.2014.02.006.
Lee, K.T., Yen, B.C., 1997. Geomorphology and kinematic-wave based hydrograph deviation. J. Hydraul. Eng. 123, 73–80. https://doi.org/10.1061/(ASCE)0733-9429(1997)123:1(73).
Lee, K.T., Cheng, N.K., Gartsman, B.I., Bugayets, A.N., 2009. A current version of the model of a unit hydrograph and its use in Taiwan and Russia. Geogr. Nat. Resour. 30 (1), 79–85. https://doi.org/10.1016/j.gnr.2009.03.015.
Marchi, L., Borga, M., Preciso, E., Gaume, E., 2010. Characterisation of selected extreme flash floods in Europe and implications for flood risk management. J. Hydrol. 394 (1–2), 118–133. https://doi.org/10.1016/j.jhydrol.2010.07.017.
Maximenko, N., Hafner, J., Niiler, P., 2012. Pathways of marine debris derived from trajectories of Lagrangian drifters. Mar. Pollut. Bull. 65, 51–62. https://doi.org/10.1016/j.marpolbul.2011.04.016.
Miladinova, S., Macias, D., Stips, A., Garcia-Gorriz, E., 2020. Identifying distribution and accumulation patterns of floating marine debris in the Black Sea. Mar. Pollut. Bull. 153, 110964. https://doi.org/10.1016/j.marpolbul.2020.110964.
Moncheva, S., Stefanova, K., Krastev, A., Apostolov, A., Bat, L., Sezgin, M., Sahin, F., Timofte, F., 2016. Marine litter quantification in the black sea: a pilot assessment. Turkish Journal of Fisheries an Aquatic Sciences 15, 22–29. https://doi.org/10.4194/1303-2712-v16_1_22.
Moore, C.J., 2008. Synthetic polymers in the marine environment: a rapidly increasing, long-term threat. Environ. Res. 108, 131–139. https://doi.org/10.1016/j.envres.2008.07.025.
Moore, E., Lyday, S., Roletto, J., Litle, K., Parrish, J.K., Nevins, H., Harvey, J., Mortenson, J., Greig, D., Piazza, M., Hermace, A., Lee, D., Adams, D., Allen, S., Kell, S., 2009. Entanglements of marine mammals and seabirds in central California and the northwest coast of the United States 2001–2005. Mar. Pollut. Bull. 58, 1045–1051. https://doi.org/10.1016/j.marpolbul.2009.02.006.
Osadchiev, A.A., 2015. A method for quantifying freshwater discharge rates from satellite observations and Lagrangian numerical modeling of river plumes. Environ. Res. Lett. 10, 085009. https://doi.org/10.1088/1748-9326/10/8/085009.
Osadchiev, A.A., 2018. Small mountainous rivers generate high-frequency internal waves in coastal ocean. Sci. Rep. 8, 16609. https://doi.org/10.1038/s41598-018-35070-7.
Osadchiev, A.A., Korshenko, E.A., 2017. Small river plumes off the north-eastern coast of the Black Sea under average climatic and flooding discharge conditions. Ocean Sci. 13, 465–482. https://doi.org/10.5194/os-13-465-201.
Osadchiev, A.A., Sedakov, R.O., 2019. Spreading dynamics of small river plumes off the northeastern coast of the Black Sea observed by Landsat 8 and Sentinel-2. Remote Sensing Environment 221, 522–533. https://doi.org/10.1016/j.rse.2018.11.043.
Ourmieres, Y., Mansui, J., Molcard, A., Galgani, F., Poitou, I., 2018. The boundary current role on the transport and stranding of floating marine litter: the French Riviera case. Cont. Shelf Res. 155, 11–20. https://doi.org/10.1016/j.csr.2018.01.010.
Page, B., McKenzie, J., McIntosh, R., Baylis, A., Morrissey, A., Calvert, N., Haase, T., Berris, M., Dowie, D., Shaughnessy, P.C., Goldsworthy, S.D., 2004. Entanglement of Australian sea lions and New Zealand fur seals in lost fishing gear and other marine debris before and after government and industry attempts to reduce the problem. Mar. Pollut. Bull. 49, 33–42. https://doi.org/10.1016/j.marpolbul.2004.01.006.
PlasticsEurope, Association of Plastics Manufacturers, Plastics – the Facts, 2019. An analysis of European plastics production, demand and waste data. Available at: https://www.plasticseurope.org/application/files/9715/7129/9584/FINAL_web_version_Plastics_the_facts2019_14102019.pdf/, Accessed date: 2 February 2020.
Polonsky, A.B., Shokurova, I.G., Belokopytov, V.N., 2013. Desjatiletnjaja Izmenchivost' Temperatury i Solenosti v Chernom More [Decadal variability of temperature and salinity in the Black Sea]. Morskoy Gidrofizicheckiy Zhurnal 6, 27–41 (in Russian).
Rech, S., Macaya-Caquilpán, V., Pantoja, J.F., Rivadeneira, M.M., Jofre Madariaga, D., Thiel, M., 2014. Rivers as a source of marine litter—a study from the SE Pacific. Mar. Pollut. Bull. 82, 66–75. https://doi.org/10.1016/j.marpolbul.2014.03.019.
Reisser, J., Shaw, J., Wilcox, C., Hardesty, B.D., Proietti, M., Thums, M., Pattiaratchi, C., 2013. Marine plastic pollution in waters around Australia: characteristics, concentrations, and pathways. PLoS One 8 (11), e80466. https://doi.org/10.1371/journal.pone.0080466.
Rochman, C.M., Hentschel, B.T., Teh, S.J., 2014. Long-term sorption of metals is similar among plastic types: implications for plastic debris in aquatic environments. PLoS One 9 (1), e85433. https://doi.org/10.1371/journal.pone.0085433.
Ryan, P.G., 2013. A simple technique for counting marine debris at sea reveals steep litter gradients between the Straits of Malacca and the Bay of Bengal. Mar. Pollut. Bull. 69, 128–136. https://doi.org/10.1016/j.marpolbul.2013.01.016.
Schmidt, C., Krauth, T., Wagner, S., 2017. Export of plastic debris by rivers into the sea. Environmental Science & Technology 51 (21), 12246–12253. https://doi.org/10.1021/acs.est.7b02368.
Simeonova, A., Chuturkova, R., Yaneva, V., 2017. Seasonal dynamics of marine litter along the Bulgarian Black Sea coast. Mar. Pollut. Bull. 119 (1), 110–118. https://doi.org/10.1016/j.marpolbul.2017.03.035.
Skamarock, W.C., Klemp, J.B., Dudhia, J., Gill, D.O., Barker, D., Duda, M.G., Huang, X.Y., Wang, W., Powers, J.G., 2008. A description of the advanced research WRF version 3. NCAR Technical Notes. https://doi.org/10.5065/D68S4MVH.
Stanev, E.V., Ricker, M., 2019. The fate of marine litter in semi-enclosed seas. Case of the Black Sea. Front. Mar. Sci. 6, 660. https://doi.org/10.3389/fmars.2019.00660.
Staneva, J., Behrens, A., Ricker, M., Gayer, G., 2020. Black Sea waves analysis and forecast (CMEMS BLK-waves 2016-present) (version 1) [data set]. In: Copernicus Monitoring Environment Marine Service (CMEMS), https://doi.org/10.25423/CMCC/BLKSEA_ANALYSIS_FORECAST_WAV_007_003.
Suaria, G., Aliani, S., 2014. Floating debris in the Mediterranean Sea. Mar. Pollut. Bull. 86 (1–2), 494–504. https://doi.org/10.1016/j.marpolbul.2014.06.025.
Suaria, G., Melinte-Dobrinescu, M.C., Ion, G., Aliani, S., 2015. First observations on the abundance and composition of floating debris in the Northwestern Black Sea. Mar. Environ. Res. 107, 45–49. https://doi.org/10.1016/j.marenvres.2015.03.011.
Terzi, Y., Seyhan, K., 2017. Seasonal and spatial variations of marine litter on the south-eastern Black Sea coast. Mar. Pollut. Bull. 120, 154–158. https://doi.org/10.1016/j.marpolbul.2017.04.041.
Topçu, E.N., Tonay, A.M., Dede, A., Öztürk, A.A., Öztürk, B., 2013. Origin and abundance of marine litter along sandy beaches of the Turkish Western Black Sea coast. Mar. Environ. Res. 85, 21–28. https://doi.org/10.1016/j.marenvres.2012.12.006.
Tsyplenkov, A.S., Golosov, V.N., Kuksina, L.V., 2017. Assessment of basin component of suspended sediment yeild generated due to rainfall events at small rivers in wet and dry subtropics. Engineering Survey (9), 54–65. https://doi.org/10.25296/1997-8650-2017-9-54-65.
UNEP, 2016. Marine Plastic Debris and Microplastics–Global Lessons and Research to Inspire Action and Guide Policy Change. United Nations Environment Programme, Nairobi.
Väli, G., Zhurbas, V.M., Laanemets, J., Lips, U., 2018. Clustering of floating particles due to submesoscale dynamics: a simulation study for the Gulf of Finland. Fundamentalnaya i prikladnaya gidrofizika 11 (2), 21–35. https://doi.org/10.7868/s2073667318020028.
Van der Wal, M., Van der Meulen, M., Tweehuijsen, G., Peterlin, M., Palatinus, A., Kovač Viršek, M., Coscia, L., Krzan, A., 2015. SFRA0025: identification and assessment of riverine input of (marine) litter. Available at. http://ec.europa.eu/environment/marine/good-environmental-status/descriptor-10/pdf/iasFinal%20Report.pdf, Accessed date: 2 February 2020.
Van Sebille, E., Aliani, S., Law, K.L., Maximenko, N., Alsina, J.M., Bagaev, A., Bergmann, M., Chapron, B., Chubarenko, I., Cózar, A., Delandmeter, P., Egger, M., Fox-Kemper, B., Garaba, S.P., Goddijn-Murphy, L., Hardesty, B.D., Hoffman, M.J., Isobe, A., Jongedijk, C.E., Kaandorp, M.L.A., Khatmullina, L., Koelmans, A.A., Kukulka, T., Laufkötter, C., Lebreton, L., Lobelle, D., Maes, C., Martinez-Vicente, V., Maqueda, M.A.M., Poulain-Zarcos, M., Rodríguez, E., Ryan, P.G., Shanks, A.L., Shim, W.J., Suaria, G., Thiel, M., Van den Bremer, T.S., Wichmann, D., 2020. The physical oceanography of the transport of floating marine debris. Environ. Res. Lett. 15, 023003. https://doi.org/10.1088/1748-9326/ab6d7d.
Veerasingam, S., Mugilarasan, M., Venkatachalapathy, R., Vethamony, P., 2016. Influence of 2015 flood on the distribution and occurrence of microplastic pellets along the Chennai coast, India. Mar. Pollut. Bull. 109, 196–204. https://doi.org/10.

1016/j.marpolbul.2016.05.082.
Volodin, E.M., Dianskii, N.A., Gusev, A.V., 2010. Simulating present-day climate with the INMCM4.0 coupled model of the atmospheric and oceanic general circulations. Izvestiya, Atmospheric and Oceanic Physics 46, 414–431. https://doi.org/10.1134/s000143381004002x.
Votier, S.C., Archibald, K., Morgan, G., Morgan, L., 2011. The use of plastic debris as nesting material by a colonial seabird and associated entanglement mortality. Mar. Pollut. Bull. 62, 168–172. https://doi.org/10.1016/j.marpolbul.2010.11.009.
Wagner, M., Scherer, C., Alvarez-Muñoz, D., Brennholt, N., Bourrain, X., Buchinger, S., Fries, E., Grosbois, C., Klasmeier, J., Marti, T., Rodriguez-Mozaz, S., Urbatzka, R., Vethaak, A.D., Winther-Nielsen, M., Reifferscheid, G., 2014. Microplastics in freshwater ecosystems: what we know and what we need to know. Environ. Sci. Eur. 26 (1), 1–9. https://doi.org/10.1186/s12302-014-0012-7. 12.
World Economic Forum, Ellen MacArthur Foundation and McKinsey & Company, 2016. The new plastics economy — rethinking the future of plastics. Available at: http://www.ellenmacarthurfoundation.org/publications, Accessed date: 2 February 2020.
Yankovsky, A.E., Chapman, D.C., 1997. A simple theory for the fate of buoyant coastal discharges. Journal of Physical Oceanogaphy 27, 1386–1401. https://doi.org/10.1175/1520-0485(1997)027<1386:ASTFTF>2.0.CO;2.
Zavialov, P.O., Makkaveev, P.N., Konovalov, B.V., Osadchiev, A.A., Khlebopashev, P.V., Pelevin, V.V., Grabovskiy, A.B., Izhitskiy, A.S., Goncharenko, I.V., Soloviev, D.M., Polukhin, A.A., 2014. Hydrophysical and hydrochemical characteristics of the sea areas adjacent to the estuaries of small rivers if the Russian coast of the Black Sea. Oceanology 54, 265–280. https://doi.org/10.1134/s0001437014030151.
Zettler, E.R., Mincer, T.J., Amaral-Zettler, L.A., 2013. Life in the “Plastisphere”: microbial communities on plastics marine debris. Environmental Science & Technology 47 (13), 7137–7146. https://doi.org/10.1021/es401288x.
Zhurbas, V.M., Kuzmina, N.P., Lyzhkov, D.A., 2017. Eddy formation behind a coastal cape in a flow generated by transient longshore wind (numerical experiment). Oceanology 57, 350–359. https://doi.org/10.1134/S0001437017020229.